Composite Structures **22** (1992) 109–120

Finite element transient analysis of composite and sandwich plates based on a refined theory and a mode superposition method

T. Kant, C. P. Arora & J. H. Varaiya

Department of Civil Engineering, Indian Institute of Technology, Powai, Bombay 400 076, India

Transient dynamic response of composite and sandwich plates is obtained using a recently developed refined shear deformation theory and mode superposition technique. The free vibration response is computed using the generalized Jacobi method with a sub-space iteration technique and then the mode shapes are used for computing the dynamic response. A special mass lumping procedure is used in the dynamic equilibrium equations. Duhamel's integral is used for the time integration of uncoupled systems. The method leads to considerable saving in computation time during computer implementation for the same order of accuracy in results as compared to direct integration methods. Numerical examples are solved for different types of dynamic loads and the results compared with those available in the literature. The mode superposition method has given good results and at the same time there is considerable saving in computer time. Unlike direct numerical integration techniques, here the time step requirements are only for obtaining the variation of displacement and stress resultants with time and for closely approximating the time dependent forcing function during numerical integration of single degree of freedom modal equations.

1 INTRODUCTION

The increasing use of fibre composite/sandwich structures in aerospace and automotive applications has generated considerable interest in this field. Due to the nature of their applications, there exists a need for assessing the transient response of composite laminated plates.

The linear elastic dynamic analysis of isotropic plates has been investigated by several researchers. Reismann and his colleagues[1–3] analysed simply supported, rectangular, thick and thin isotropic plates. Hinton[4] used central difference time integration and quadratic axisymmetric one-dimensional elements for linear elastic dynamic analysis of circular plates and obtained good results. He included the effects of rotary inertia and transverse shear energy in the formulation. Pica & Hinton[5] presented a unified approach to static and dynamic linear and geometrically non-linear analysis of Mindlin plates including initial imperfections. A finite element idealization was adopted using a nine-node quadratic Mindlin plate element with selective reduced integration. An explicit central difference technique was used for time stepping and the results were reported for specific applications. Later they presented[6] further developments in this unified approach to the static and dynamic non-linear analysis of Mindlin plates. The diagonal mass matrix formulation has proved to be more effective and generally as accurate as the consistent mass matrix.

For the dynamic analysis of composite plates, Mindlin's homogeneous isotropic plate theory has been extended to laminated plates by Yang *et al.*[7] and by Whitney & Pagano.[8] Using Mindlin plate theory, Moon[9] investigated the response of infinite laminated plates subjected to transverse impact loads at the centre of the plate. Wang *et al.*[10] applied method of characteristics to investigate the dynamic response of symmetric orthotropic plates. Sun & Whitney[11–13] applied the classical method of separation of variables combined with a Mindlin–Goodman[14] procedure for treating time dependent boundary conditions and/or dynamic external loadings on plates under cylindrical bending.

Composite Structures 0263-8223/92/$05·00

Rock & Hinton[15] used Newmark's method for finding the transient response of thick and thin plates. Akay[16] used the same method for dynamic large deflection analysis of Reissner plates using a mixed finite element method and has shown that it loses its unconditional stability in non-linear analysis. Reddy[17-18] used Newmark's integration scheme for the forced response of rectangular composite plates with cross ply and angle ply lamination schemes and also for transient analysis of orthotropic plates based on first order shear deformable theory (FOST).

In the present work, a higher order shear deformation theory (HOST) developed by one of the present authors[19-24] is employed to investigate the transient response of isotropic and layered anisotropic composite plates. The finite element method for space idealization is adopted and the nine-node quadratic Lagrangian element is used with selective reduced integration. For computing the transient dynamic response, the method of mode superposition is used. To the authors' knowledge, it is the first time that this method has been employed for the dynamic analysis of composite/sandwich plates. The generalized Jacobi method with a sub-space iteration technique is being used for the free vibration analysis[20] which seems to be more accurate, economical and versatile. The damping effects are ignored. A diagonal mass matrix with special mass lumping is employed for the analysis.[25] The transient response study is done for various types of dynamic loads, namely, pulse and blast loads. Numerical results are presented and compared with the results from other sources reported in the literature. The procedure is found to give good performance for all the problems and there is considerable saving on account of computation time on computer implementation.

2 THEORETICAL FORMULATION

The present higher order shear deformation theory is based on the displacement model (see Fig. 1).

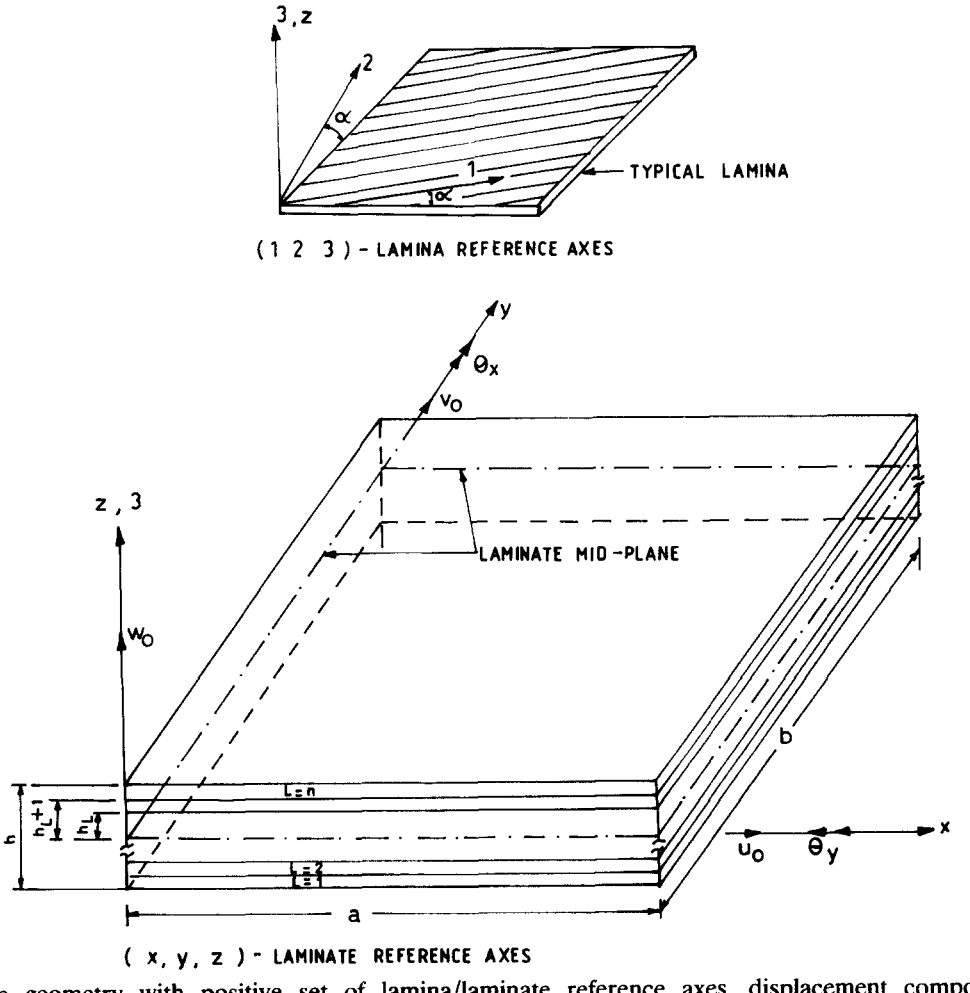

Fig. 1. Laminate geometry with positive set of lamina/laminate reference axes, displacement components and fibre orientation.

$$
\begin{aligned}
u(x,y,z,t) &= u_0(x,y,t) + z\theta_x(x,y,t) + z^2 u_0^*(x,y,t) \\
&\quad + z^3\theta_x^*(x,y,t) \\
v(x,y,z,t) &= v_0(x,y,t) + z\theta_y(x,y,t) \\
&\quad + z^2 v_0^*(x,y,t) \\
&\quad + z^3\theta_y^*(x,y,t) \\
w(x,y,z,t) &= w_0(x,y,t)
\end{aligned} \tag{1}
$$

where t is time, u_0, v_0 and w_0 are the inplane and transverse displacements of a point (x,y) on the mid-plane respectively and θ_x, θ_y are the rotations of the normal to the mid-plane about the y and x axes respectively. The parameters u_0^*, v_0^*, θ_x^* and θ_y^* are the coresponding higher order deformation terms in the Taylor series expansion and are also defined at the mid-plane. The parameters u, v and w are the displacement components in the x, y and z directions respectively of a generic point in the laminate space.

The strains associated with the displacements in eqn (1) are as follows:

$$
\begin{aligned}
\varepsilon_x &= \varepsilon_{x0} + z\kappa_x + z^2\varepsilon_{x0}^* + z^3\kappa_x^* \\
\varepsilon_y &= \varepsilon_{y0} + z\kappa_y + z^2\varepsilon_{y0}^* + z^3\kappa_y^* \\
\varepsilon_z &= 0 \\
\varepsilon_{xy} &= \varepsilon_{xy0} + z\kappa_{xy} + z^2\varepsilon_{xy0}^* + z^3\kappa_{xy}^* \\
\gamma_{yz} &= \phi_y + z\psi_y + z^2\phi_y^* \\
\gamma_{xz} &= \phi_x + z\psi_x + z^2\phi_x^*
\end{aligned} \tag{2a}
$$

where

$$
\begin{aligned}
\boldsymbol{\varepsilon}_0 &= [\varepsilon_{x0}, \varepsilon_{y0}, \varepsilon_{xy0}]^{\mathrm{T}} \\
&= \left[\frac{\partial u_0}{\partial x}, \frac{\partial v_0}{\partial y}, \frac{\partial u_0}{\partial y} + \frac{\partial v_0}{\partial x}\right]^{\mathrm{T}} \\
\boldsymbol{\varepsilon}_0^* &= [\varepsilon_{x0}^*, \varepsilon_{y0}^*, \varepsilon_{xy0}^*]^{\mathrm{T}} \\
&= \left[\frac{\partial u_0^*}{\partial x}, \frac{\partial v_0^*}{\partial y}, \frac{\partial u_0^*}{\partial y} + \frac{\partial v_0^*}{\partial x}\right]^{\mathrm{T}} \\
\boldsymbol{\kappa} &= [\kappa_x, \kappa_y, \kappa_{xy}]^{\mathrm{T}} \\
&= \left[\frac{\partial \theta_x}{\partial x}, \frac{\partial \theta_y}{\partial y}, \frac{\partial \theta_x}{\partial y} + \frac{\partial \theta_y}{\partial x}\right]^{\mathrm{T}} \\
\boldsymbol{\kappa}^* &= [\kappa_x^*, \kappa_y^*, \kappa_{xy}^*]^{\mathrm{T}} \\
&= \left[\frac{\partial \theta_x^*}{\partial x}, \frac{\partial \theta_y^*}{\partial y}, \frac{\partial \theta_x^*}{\partial y} + \frac{\partial \theta_y^*}{\partial x}\right]^{\mathrm{T}}
\end{aligned} \tag{2b}
$$

$$
\boldsymbol{\phi} = [\phi_x, \phi_y]^{\mathrm{T}} = \left[\theta_x + \frac{\partial w_0}{\partial x}, \theta_y + \frac{\partial w_0}{\partial y}\right]^{\mathrm{T}}
$$

$$
\boldsymbol{\phi}^* = [\phi_x^*, \phi_y^*]^{\mathrm{T}} = [3\theta_x^*, 3\theta_y^*]^{\mathrm{T}}
$$

$$
\boldsymbol{\psi} = [\psi_x, \psi_y]^{\mathrm{T}} = [2u_0^*, 2v_0^*]^{\mathrm{T}}
$$

and T represents the transpose of an array.

The generalized strain vector $\bar{\boldsymbol{\varepsilon}}$ corresponding to the middle surface may be written as

$$
\begin{aligned}
\bar{\boldsymbol{\varepsilon}} = [&\varepsilon_{x0}, \varepsilon_{y0}, \varepsilon_{xy0}, \varepsilon_{x0}^*, \varepsilon_{y0}^*, \varepsilon_{xy0}^*, \kappa_x, \kappa_y, \kappa_{xy}, \\
&\kappa_x^*, \kappa_y^*, \kappa_{xy}^*, \phi_x, \phi_y, \psi_x, \psi_y, \phi_x^*, \phi_y^*]^{\mathrm{T}}
\end{aligned} \tag{3}
$$

Following the usual transformation rule[26] of the stress–strain in lamina and laminate coordinate systems, the stress–strain relations for the Lth lamina in the laminate coordinates $(x\text{–}y\text{–}z)$ are written as

$$
\begin{bmatrix} \sigma_x \\ \sigma_y \\ \tau_{xy} \\ \tau_{yz} \\ \tau_{xz} \end{bmatrix}^L
= \begin{bmatrix}
Q_{11} & Q_{12} & Q_{13} & 0 & 0 \\
 & Q_{22} & Q_{23} & 0 & 0 \\
 & & Q_{33} & 0 & 0 \\
 & & & Q_{44} & Q_{45} \\
\text{SYM.} & & & & Q_{55}
\end{bmatrix}^L
\begin{bmatrix} \varepsilon_x \\ \varepsilon_y \\ \gamma_{xy} \\ \gamma_{yz} \\ \gamma_{xz} \end{bmatrix}^L \tag{4a}
$$

or

$$
\boldsymbol{\sigma} = \mathbf{Q}\boldsymbol{\varepsilon} \tag{4b}
$$

in which $\boldsymbol{\sigma}$ and $\boldsymbol{\varepsilon}$ are the stress and linear strain vectors with respect to the laminate axes and the Q_{ij}s are the reduced elastic constants in the laminate axes of the L th lamina.

2.1 Equations of motion

The Hamilton variational principle is used here to derive the laminate equations of motion. The mathematical statement of the Hamilton principle in the absence of damping can be written as,

$$
\int_{t_1}^{t_2} \delta(\Pi - E)\,\mathrm{d}t = 0 \tag{5}
$$

where Π and E are the total potential energy and the kinetic energy respectively.

The potential energy Π of the plate with volume V and surface area A can be written as

$$
\Pi = U - W
$$

or

$$\Pi = 1/2 \int_V \boldsymbol{\varepsilon}^T \boldsymbol{\sigma}\, dv - \int_V \mathbf{u}^T \mathbf{p}\, dv \tag{6}$$

where U is the strain energy of the plate, W represents the work done by externally applied forces, $\mathbf{p}$ is the vector of the force intensities corresponding to laminate direction (x,y,z) and $\mathbf{u}=[u,v,w]^T$ is the displacement of any generic point (x,y,z) in space. The expressions for strain components given by eqn (2) are substituted in energy expression (6). An explicit integration through the laminate thickness is then carried out to obtain the following expression

$$\Pi = 1/2 \int_A \bar{\boldsymbol{\varepsilon}}^T \bar{\boldsymbol{\sigma}}\, dA - \int_A \mathbf{d}^T \mathbf{F}\, dA \tag{7}$$

in which $\mathbf{F}$ is a vector of load per unit area corresponding to mid-plane displacement vector $\mathbf{d}$ and $\bar{\boldsymbol{\sigma}}$ is the stress resultant vector as derived in Ref. 19, and the relation between stress resultant and generalized strain vector can be concisely expressed as

$$\bar{\boldsymbol{\sigma}} = \mathbf{D}\bar{\boldsymbol{\varepsilon}} \tag{8}$$

or

$$\begin{pmatrix} \mathbf{N}^* \\ \mathbf{N}^* \\ \hline \mathbf{M} \\ \mathbf{M}^* \\ \hline \mathbf{Q} \\ \mathbf{S} \\ \mathbf{Q}^* \end{pmatrix} = \left(\begin{array}{c|c|c} \mathbf{D}_m & \mathbf{D}_c & 0 \\ \hline \mathbf{D}_c^T & \mathbf{D}_b & 0 \\ \hline 0 & 0 & \mathbf{D}_s \end{array}\right) \begin{pmatrix} \boldsymbol{\varepsilon}_0 \\ \boldsymbol{\varepsilon}_0^* \\ \hline \boldsymbol{\kappa} \\ \boldsymbol{\kappa}^* \\ \hline \boldsymbol{\phi} \\ \boldsymbol{\psi} \\ \boldsymbol{\phi}^* \end{pmatrix} \tag{9}$$

Thus, with the assumed displacement model, the various rigidity matrices derived are

$\mathbf{D}_m$: membrane; $\mathbf{D}_c$: membrane–flexure coupling

$\mathbf{D}_b$: flexure; $\mathbf{D}_s$: shear.

2.1.1 Interlaminar stresses

The interlaminar transverse stresses (τ_{xz}, τ_{yz}, σ_z) cannot be accurately estimated by eqn (4). This is mainly due to the fact that the constitutive laws are discontinuous across the laminae interfaces whereas interlaminar stresses have to maintain continuity across the interfaces. For these reasons, the interlaminar stresses between the layers 'L' and '$L+1$' are obtained by integrating the following three equilibrium equations of three-dimensional elasticity for each layer over the lamina thickness and summing over layer 1 to 'L'.

$$\begin{aligned} \frac{\partial \sigma_x}{\partial x} + \frac{\partial \tau_{xy}}{\partial y} + \frac{\partial \tau_{xz}}{\partial z} &= 0 \\ \frac{\partial \tau_{xy}}{\partial x} + \frac{\partial \sigma_y}{\partial y} + \frac{\partial \tau_{yz}}{\partial z} &= 0 \\ \frac{\partial \tau_{xz}}{\partial x} + \frac{\partial \tau_{yz}}{\partial y} + \frac{\partial \sigma_z}{\partial z} &= 0 \end{aligned} \tag{10}$$

The above equilibrium equations without body forces are rewritten in the following form for computation.

$$\begin{aligned} \tau^L_{xz|z=h_{L+1}} &= -\sum_{i=1}^{L} \int_{h_i}^{h_{i+1}} \left(\frac{\partial \sigma_x^i}{\partial x} + \frac{\partial \tau_{xy}^i}{\partial y} \right) dz \\ \tau^L_{yz|z=h_{L+1}} &= -\sum_{i=1}^{L} \int_{h_i}^{h_{i+1}} \left(\frac{\partial \sigma_y^i}{\partial y} + \frac{\partial \tau_{xy}^i}{\partial x} \right) dz \\ \sigma^L_{z|z=h_{L+1}} &= -\sum_{i=1}^{L} \int_{h_i}^{h_{i+1}} \left(\frac{\partial \tau_{xz}^i}{\partial x} + \frac{\partial \tau_{yz}^i}{\partial y} \right) dz \end{aligned} \tag{11}$$

2.1.2 Kinetic energy expression

The kinetic energy of the body is given by

$$E = 1/2 \int_v \dot{\mathbf{u}}^T \rho \dot{\mathbf{u}}\, dv \tag{12a}$$

where $\mathbf{u}=[u,v,w]^T$ is the displacement of any generic point (x,y,z) in space, $\dot{\mathbf{u}}$ is the corresponding velocity vector and ρ is the mass density of the material. The expression for $\mathbf{u}$ is substituted in eqn (12a) using eqn (1) and on carrying out explicit integration through the thickness of the laminate, this relation can be reduced to a two-dimensional form as

$$E = 1/2 \int_A \dot{\mathbf{d}}^T \bar{m} \dot{\mathbf{d}}\, dA \tag{12b}$$

where the inertia matrix $\bar{m}$ is given as,

$$\bar{m} = \begin{bmatrix} I_0 & 0 & 0 & I_1 & 0 & I_2 & 0 & I_3 & 0 \\ 0 & I_0 & 0 & 0 & I_1 & 0 & I_2 & 0 & I_3 \\ 0 & 0 & I_0 & 0 & 0 & 0 & 0 & 0 & 0 \\ I_1 & 0 & 0 & I_2 & 0 & I_3 & 0 & I_4 & 0 \\ 0 & I_1 & 0 & 0 & I_2 & 0 & I_3 & 0 & I_4 \\ I_2 & 0 & 0 & I_3 & 0 & I_4 & 0 & I_5 & 0 \\ 0 & I_2 & 0 & 0 & I_3 & 0 & I_4 & 0 & I_5 \\ I_3 & 0 & 0 & I_4 & 0 & I_5 & 0 & I_6 & 0 \\ 0 & I_3 & 0 & 0 & I_4 & 0 & I_5 & 0 & I_6 \end{bmatrix} \tag{12c}$$

in which

$$I_i = \sum_{L=1}^{NL} \int_{h_L}^{h_{L+1}} z^i \rho^L \, dz \quad i = 0,6 \tag{12d}$$

and ρ^L is the material density of the Lth layer. Here, $\bar{m}$ defines the generalized mass matrix of the laminate under consideration.

The substitution of eqns (7), (8) and (12) into the mathematical statement of the Hamilton principle gives,

$$\delta \int_{t_1}^{t_2} \left[1/2 \int_A \bar{\boldsymbol{\varepsilon}}^T \mathbf{D} \bar{\boldsymbol{\varepsilon}} \, dA - \int_A \mathbf{d}^T \mathbf{F} \, dA - 1/2 \int_A \dot{\mathbf{d}}^T \bar{m} \dot{\mathbf{d}} \, dA \right] = 0 \tag{13}$$

The application of this principle furnishes the equations of motion of any given system.

3 FINITE ELEMENT DISCRETIZATION

In standard finite element techniques, the continuum displacement vector within the element is discretized such that

$$\mathbf{d}(t) = \sum_{i=1}^{NN} N_i(x,y) \, \mathbf{d}_i(t) \tag{14}$$

where N_i is the interpolation function corresponding to node i, NN is the number of nodes in the element and $\mathbf{d}_i$ is the vector of the nodal degrees of freedom corresponding to node i, such that

$$\mathbf{d}_i = [u_{0i}, v_{0i}, w_{0i}, \theta_{xi}, \theta_{yi}, u^*_{0i}, v^*_{0i}, \theta^*_{xi}, \theta^*_{yi}]^T \tag{15}$$

Knowing the generalized displacement vector $\mathbf{d}$ at all points within the element, the generalized strain at any point, given by eqns (2), can be expressed in matrix form as follows:

$$\bar{\boldsymbol{\varepsilon}} = \sum_{i=1}^{NN} \mathbf{B}_i \, \mathbf{d}_i \tag{16}$$

Equation (16) can also be written in an alternate form as

$$\bar{\boldsymbol{\varepsilon}} = \mathbf{B} \mathbf{a}_e \tag{17a}$$

in which,

$$\mathbf{B} = [\mathbf{B}_1, \mathbf{B}_2, \ldots, \mathbf{B}_{NN}] \tag{17b}$$

The strain–displacement matrix B_i, is defined elsewhere.[22]

For any approximate discretization scheme in space, the dynamic problem in the absence of damping invariably gives rise to a set of ordinary differential equations of the form

$$\mathbf{M}\ddot{\mathbf{a}} + \mathbf{K}\mathbf{a} = \mathbf{f}(\mathbf{t}) \tag{18}$$

in which $\ddot{\mathbf{a}}$, $\mathbf{a}$ are the global vectors of unknown acceleration and displacement respectively. The global stiffness matrix $\mathbf{K}$, the global mass matrix $\mathbf{M}$ and the global nodal force vector $\mathbf{f}(t)$ are computed in the usual manner as follows:

$$\mathbf{M} = \sum_{e=1}^{NE} \mathbf{M}_e$$

$$\mathbf{K} = \sum_{e=1}^{NE} \mathbf{K}_e \tag{19}$$

$$\mathbf{f}(t) = \sum_{e=1}^{NE} \mathbf{f}_e(t)$$

4 DYNAMIC ANALYSIS USING MODE SUPERPOSITION METHOD

4.1 Decoupling of equations and integration

The finite element equations in eqn (18) are generally coupled, with banded $\mathbf{K}$ and either banded or diagonal $\mathbf{M}$. They would be uncoupled if and only if both the matrices $\mathbf{K}$ and $\mathbf{M}$ were diagonal. A system of uncoupled ordinary differential equations is considerably less expensive to integrate than a coupled system. The purpose of mode superposition is to transform eqn (18) into an uncoupled form in order to make the procedure cost efficient. The transformation adds to the computation cost, but in many situations this cost is more than offset by the subsequent saving in dealing with a computationally more efficient system. Such a situation occurs in dynamic analysis when the time history is required for a relatively longer time duration (i.e. at a large number of time steps).

The undamped modes for eqn (18) are time harmonic (sinusoidal) solutions when there are no loads ($\mathbf{f} = \mathbf{0}$) and when damping is neglected, i.e.

$$\mathbf{M}\ddot{\mathbf{a}} + \mathbf{K}\mathbf{a} = \mathbf{0} \tag{20}$$

The solution to eqn (20) can be postulated to be of the form:

$$\mathbf{a} = \boldsymbol{\phi} \, e^{i\omega t} \tag{21}$$

where $e^{i\omega t} = \cos \omega t + i \sin \omega t$ is a complex notation for a sinusoidal time variation. Substitution of eqn (21) into eqn (20) yields

$$\mathbf{K}\boldsymbol{\phi} - \omega^2 \mathbf{M}\boldsymbol{\phi} = \mathbf{0} \tag{22a}$$

which is a generalized eigenvalue problem where the eigenvalue λ is the square of the circular frequency,

$$\lambda = \omega^2 \tag{22b}$$

K and **M** are generally real, symmetric and positive definite. Thus, if the system has N active degrees of freedom, i.e. the number of degrees of freedom not constrained by zero-valued essential boundary conditions, then there are n eigensolutions:

$$(\omega_1^2, \boldsymbol{\phi}_1), (\omega_2^2, \boldsymbol{\phi}_2), \ldots, (\omega_n^2, \boldsymbol{\phi}_n) \tag{23a}$$

where

$$0 \le \omega_1 \le \omega_2 \le \omega_3 \ldots \le \omega_n \tag{23b}$$

The vector $\boldsymbol{\phi}_i$ is called the ith mode shape vector, and ω_i the corresponding frequency of vibration (rad/s). An important factor which is the basis of multidegrees of freedom analysis, is that the complete motion of the system may be obtained by superimposing the independent motions of individual modes. This forms the basis of the mode superposition method approach of dynamic analysis. The eigenvectors are orthogonal with respect to **K** and **M** and they are orthonormal with respect to **M**. An $n \times n$ square matrix $\boldsymbol{\Phi}$ that contains eigenvectors as columns can be defined as

$$\boldsymbol{\Phi} = [\boldsymbol{\phi}_1, \boldsymbol{\phi}_2, \boldsymbol{\phi}_3, \ldots, \boldsymbol{\phi}_n] \tag{24}$$

and an $n \times n$ diagonal matrix $\boldsymbol{\Omega}^2$ that contains the n eigenvalues on the diagonal as

$$\boldsymbol{\Omega}^2 = \begin{bmatrix} \omega_1^2 & & & & 0 \\ & \omega_2^2 & & & \\ & & \omega_3^2 & & \\ & & & \ddots & \\ 0 & & & & \omega_n^2 \end{bmatrix} \tag{25}$$

Using this notation, the n solutions to the generalized eigenvalue problem in eqn (22a) can be expressed as follows:

$$\mathbf{K}\boldsymbol{\Phi} = \mathbf{M}\boldsymbol{\Phi}\boldsymbol{\Omega}^2 \tag{26}$$

and the orthogonality relations may be written as

$$\boldsymbol{\Phi}^{\mathrm{T}}\mathbf{K}\boldsymbol{\Phi} = \boldsymbol{\Omega}^2$$

and

$$\boldsymbol{\Phi}^{\mathrm{T}}\mathbf{M}\boldsymbol{\Phi} = \mathbf{I} \tag{27}$$

where **I** is the identity matrix of order n.

This system of n modes can now be used to transform the system of eqns (18). The general solution to eqn (18) may be written as a linear superposition of the n modes, each multiplied by a general time varying amplitude x_i

$$\mathbf{a}(t) = \sum_{i=1}^{N} x_i(t)\boldsymbol{\phi}_i \tag{28a}$$

or

$$\mathbf{a} = \boldsymbol{\Phi}.\mathbf{X} \tag{28b}$$

and

$$\ddot{\mathbf{a}} = \boldsymbol{\Phi}.\ddot{\mathbf{X}} \tag{28c}$$

In this equation the mode shape matrix $\boldsymbol{\Phi}$ serves to transform the generalized coordinates **X** to the geometric coordinates **a**. These modal generalized coordinates are called normal coordinates of the structure. Premultiplying eqn (18) by $\boldsymbol{\Phi}^{\mathrm{T}}$ yields

$$\boldsymbol{\Phi}^{\mathrm{T}}\mathbf{M}\ddot{\mathbf{a}} + \boldsymbol{\Phi}^{\mathrm{T}}\mathbf{K}\mathbf{a} = \boldsymbol{\Phi}^{\mathrm{T}}\mathbf{f}(t) \tag{29}$$

Thus, putting eqns (27) and (28) in eqn (29), the relation becomes

$$\boldsymbol{\Phi}^{\mathrm{T}}\mathbf{M}\boldsymbol{\Phi}\ddot{\mathbf{X}} + \boldsymbol{\Phi}^{\mathrm{T}}\mathbf{K}\boldsymbol{\Phi}\mathbf{X} = \boldsymbol{\Phi}^{\mathrm{T}}.\mathbf{f}(t)$$

or

$$\mathbf{I}\ddot{\mathbf{X}} + \boldsymbol{\Omega}^2\mathbf{X} = \boldsymbol{\Phi}^{\mathrm{T}}\mathbf{f}(t) \tag{30}$$

i.e.

$$\ddot{\mathbf{X}} + \boldsymbol{\Omega}^2.\mathbf{X} = \mathbf{r}(t)$$

where $r_i(t)$ is the generalized load vector. Eqn (30) gives n independent equations of the form:

$$\text{where} \quad \left.\begin{aligned} \ddot{x}_i(t) + \omega^2 x_i(t) &= r_i(t) \\ r_i(t) &= \boldsymbol{\phi}_i^{\mathrm{t}}.\,\mathbf{f}(t) \end{aligned}\right\} \; i = 1, 2, \ldots, n \tag{31}$$

Thus, the ith typical equation in eqn (30) is the equilibrium equation of a single degree of freedom system with unit mass and stiffness ω^2. The initial conditions of motion of this system are obtained from the following expressions:

$$\left.\begin{aligned} \mathbf{X} &= \boldsymbol{\Phi}^{\mathrm{T}}\mathbf{M}\mathbf{a} \\ \ddot{\mathbf{X}} &= \boldsymbol{\Phi}^{\mathrm{T}}\mathbf{M}\ddot{\mathbf{a}} \end{aligned}\right. \tag{32}$$

and for the ith degree of freedom, it becomes

$$x_0 = \phi^T M a_0 \qquad (33)$$
$$\ddot{x}_0 = \phi^T M \ddot{a}_0$$

The solution of each equation in eqn (31) can be obtained by any of the direct integration methods or can be calculated using the Duhamel's integral as done in the present case.

4.2 Remarks

For many kinds of practical loadings, only a fraction of the total number of decoupled equations need to be considered in order to make a good approximation of the actual response to the loading. Most frequently, only the first p equilibrium equations need be used. This means that the solution for only the lower p eigenvalues and the corresponding eigenvectors is needed and the response in the first p modes only is to be summed up. This fact makes the method very cost efficient regarding computer implementation as compared to direct integration methods. The saving in computer time is enormous if the response at a large number of time steps is required.

Another very important advantage of the mode superposition technique is that there is no restriction on the length of the time step to be taken whereas direct integration procedures become either unstable or inaccurate at larger time steps. Here the time step has to be so chosen as to depict clearly the variation of displacement and other stress resultants with time and to model the time dependent forcing function for the system accurately.

The limitation of this method is that it is applicable for linear dynamic problems only and nonlinearity cannot be considered.

5 NUMERICAL RESULTS AND DISCUSSION

5.1 Preliminary remarks

For the complete analysis involving variation of stress resultants along the dimensions of the laminate, the mode superposition method requires the discretization of a full plate. This leads to slower convergence with an increase in the number of modes but when the stress resultants are required only at or near the centre, only a quarter of the laminate need be discretized with symmetric boundary conditions along the centre line[27] to obtain rapid convergence. Depending upon the requirements of the problem, full or quarter plate is considered for computing the transient response.

The following set of data and boundary conditions were used:

DATA 1

Square plate, $a = b = 25$ cm, $h = 5$ cm, $q_0 = 10$ N/cm^2

$E_2 = 2{\cdot}1 \times 10^6$ N/cm^2, $\rho = 8 \times 10^{-6}$ N-s^2/cm^4

$\nu_{12} = \nu_{23} = \nu_{13} = 0{\cdot}25$

DATA 2

Square plate, $a = b = 100$ cm, $h = 10$ cm, $q_0 = 10$ N/cm^2.

For face sheets,

$E_1 = 13{\cdot}08 \times 10^6$ N/cm^2, $E_2 = E_3 = 1{\cdot}06 \times 10^6$ N/cm^2

$G_{12} = G_{13} = 0{\cdot}6 \times 10^6$ N/cm^2, $G_{23} = 0{\cdot}39 \times 10^6$ N/cm^2

$\nu_{12} = \nu_{13} = 0{\cdot}28$, $\nu_{23} = 0{\cdot}34$

$\rho = 15{\cdot}8 \times 10^{-6}$ N-s^2/cm^4

For the core,

$G_{23} = 1{\cdot}772 \times 10^4$ N/cm^2, $G_{13} = 5{\cdot}206 \times 10^4$ N/cm^2

$\rho = 0{\cdot}1009 \times 10^{-5}$ N-s^2/cm^4

DATA 3

Square plate, $a = b = 140$ mm, $h = 4{\cdot}29$ mm

$E_1 = 40{\cdot}0 \times 10^9$ N/m^2, $E_2 = 8{\cdot}27 \times 10^9$ N/m^2

$G_{12} = G_{13} = 4{\cdot}13 \times 10^9$ N/m^2, $G_{23} = 0{\cdot}03 \times 10^9$ N/m^2

$\rho = 1901{\cdot}5$ kg/m^3, $\nu_{12} = 0{\cdot}25$

Projectile impact with initial velocity $v_0 = 22{\cdot}6$ m/s

Diameter of the impact area = 0·9525 cm

Length of the projectile = 2·54 cm

Mass of the projectile = 0·1417 kg

5.2 Boundary conditions

Simply supported

Along x-axis $u_0 = w_0 = \theta_x = u_0^* = \theta_x^* = 0$

Along y-axis $v_0 = w_0 = \theta_y = v_0^* = \theta_y^* = 0$

Clamped

Along all the edges the conditions are

$u_0 = v_0 = w_0 = \theta_x = \theta_y = u_0^* = v_0^* = \theta_x^* = \theta_y^* = 0$

Along the centre line in the case of a quarter plate symmetric boundary conditions have been taken as follows:

Along x-axis $v_0 = \theta_y = v_0^* = \theta_y^* = 0$

Along y-axis $u_0 = \theta_x = u_0^* = \theta_x^* = 0$

5.3 Examples and discussion

Example 1

Using DATA 1, a 0°/90°/0°/90°/..., cross ply simply supported along all edges with

$$E_1/E_2 = E_1/E_3, G_{12} = G_{13} = 0{\cdot}5E_2, G_{23} = 0{\cdot}2E_2$$

under a spatially sinusoidal loading of peak value of q_0 is solved using full plate discretization (2 × 2 mesh) for analysis. The results obtained are compared with closed form[17] and other reported results[24] in Table 1. It is seen that, for same total thickness, the central deflection decreases on increase in the number of layers in the laminate and on increasing E_1 for the same value of E_2.

Example 2

A 0°/90°/90°/0° composite laminate is analysed for dynamic response under a suddenly applied uniformly distributed pulse load of q_0 for Data 1. For this problem we have taken

$$E_1/E_2 = E_1/E_3 = 25, G_{12} = G_{13} = 0{\cdot}5E_2,$$
$$G_{23} = 0{\cdot}2E_2$$

Figure 2 shows the variation of the central deflection, and Fig. 3 the variation of central normal stress with time. Figure 4 shows the convergence of central normal stress σ_x(top) with increasing number of modes and refining the mesh in the analysis. A quarter plate is discretized for the analyses of all the cases in this problem. Table 2 shows the frequencies included and their effect towards the peak response.

Example 3

For a square two layered 0°/90° cross ply, simply supported composite plate, transient analysis is done for a suddenly applied pulse load using DATA 1 and other properties as specified in

Table 1. Comparison of maximum central deflection $w \times 10^3$ cm for a layered 0°/90°/0°/90°/...laminate (example 1). Data 1, $G_{12} = G_{13} = 0{\cdot}5E_2$, $G_{23} = 0{\cdot}2E_2$

E_1/E_2	Source	Number of layers			
		1	3	5	7
25	CFS [17]	0·3566 (90)	0·3386 (85)	0·2924 (80)	0·2817 (80)
	CPT [17]	0·1272 (55)	0·1272 (55)	0·1272 (55)	0·1272 (55)
	FOST [24]	0·3484 (85)	0·3309 (83)	0·2902 (77)	0·2796 (75)
	HOST [24]	0·3582 (90)	0·3399 (85)	0·2929 (80)	0·2825 (80)
	Present[a]	0·3479 (85)	0·3328 (85)	0·2903 (80)	0·2801 (75)
40	CFS [17]	0·3233 (85)	0·2985 (80)	0·2463 (70)	0·2366 (70)
	FOST [24]	0·3243 (82)	0·2993 (78)	0·2473 (70)	0·2376 (69)
	HOST [24]	0·3129 (81)	0·2907 (77)	0·2474 (71)	0·2362 (69)
	Present[a]	0·3113 (80)	0·2909 (80)	0·2453 (70)	0·2349 (70)

Bracketed figures indicate the time in μs at which these maximum values occur.
[a]A time step of 5 μs has been used for the present results. The full plate has been discretized into a 2 × 2 mesh and first nine modes have been included in the analysis.

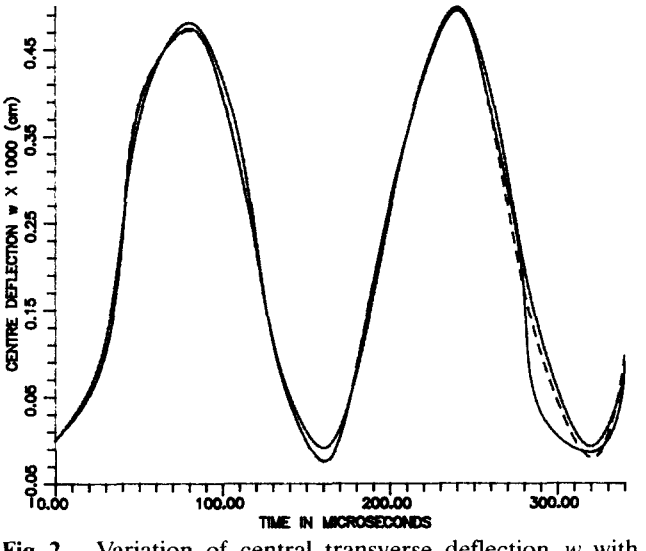

Fig. 2. Variation of central transverse deflection w with time for a 0°/90°/90°/0° plate for various mesh sizes under uniformly distributed pulse load. (·····) 1 element; (——) 2 × 2 mesh; (– – –) 3 × 3 mesh.

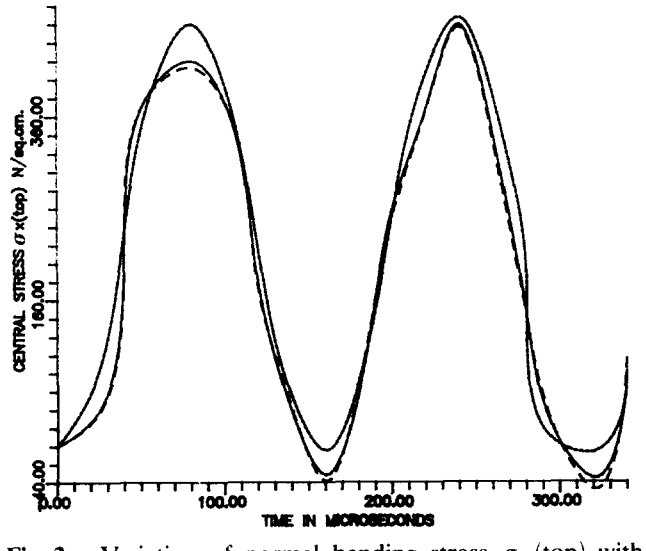

Fig. 3. Variation of normal bending stress σ_x (top) with time for a 0°/90°/90°/0° plate for various mesh sizes under uniformly distributed pulse load. (·····) 1 element; (——) 2 × 2 mesh; (– – –) 3 × 3 mesh.

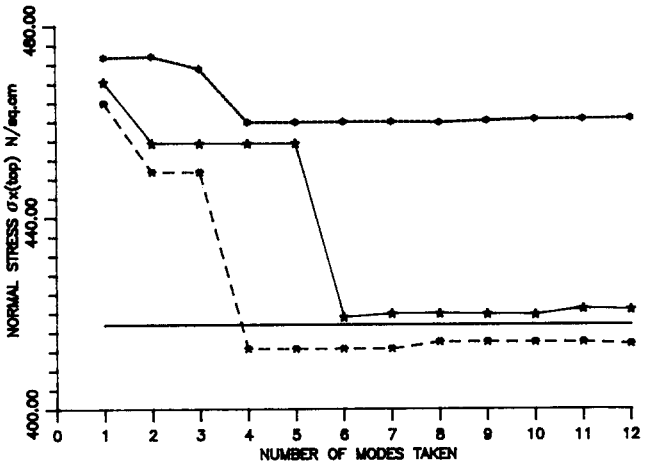

Fig. 4. Convergence of normal bending stress σ_x (top) with increase in number of modes for a 0°/90°/90°/0° plate (Data 1).

Table 2. Frequencies included in the analysis of 0°/90°/90°/0° plate (example 2) and their effect on the peak values of deflection, moment (M_x) and central normal stress (σ_x). (Reported values occurred at $t = 80\ \mu$s, $\Delta t = 20\ \mu$s.)

Nmode	Frequency (rad/s)	$w \times 10^3$ (cm)	Moment (M_x) (N-cm/cm)	Stress (σ_x) (N/cm^2)
1	39889·78	0·501 12	1428·34	468·356
2	101789·5	0·485 51	1391·34	455·468
3	120542·1	0·485 48	1391·34	455·468
4	120705·0	0·485 48	1391·39	455·409
5	121553·2	0·485 95	1391·40	455·421
6	126968·7	0·472 64	1334·30	419·172
7	149078·3	0·472 91	1335·41	419·903
8	163410·3	0·472 91	1335·41	419·903
9	173754·5	0·472 91	1335·46	419·813
10	175191·4	0·472 89	1335·34	419·700
11	178657·8	0·474 64	1336·72	420·918
12	184589·5	0·474 88	1338·11	420·726

Example 2. The results along with comparison with reported results[22] are shown in Figs 5 and 6. Table 3 gives a comparison of laminae and inter-laminar shear stresses τ_{xy} and τ_{xz} respectively with reported results.

Example 4

To validate further the application of the mode superposition method to the transient response of composite/sandwich plates, a recently reported problem of projectile impact on a laminated composite plate[28] has been solved (DATA 3). The forcing function in this case is given by Hertz's law of impact:

$$F = H(r - w)^P$$

which acts on a circular area of diameter equal to the diameter of the projectile (0·952 5 cm) at the centre of the plate. Here H is a constant whose

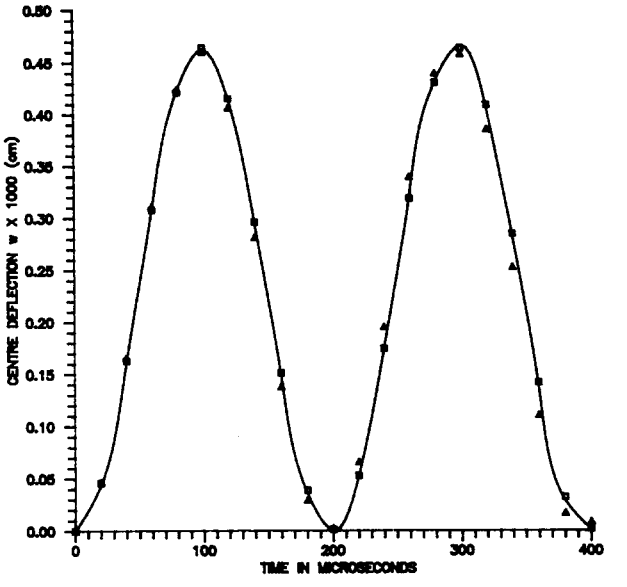

Fig. 5. Variation of central transverse deflection with time for a simply supported 0°/90° composite plate (Data 1) under suddenly applied spatially sinusoidal load. △, Mindlin;[17] □, host 11;[22] ——, present.

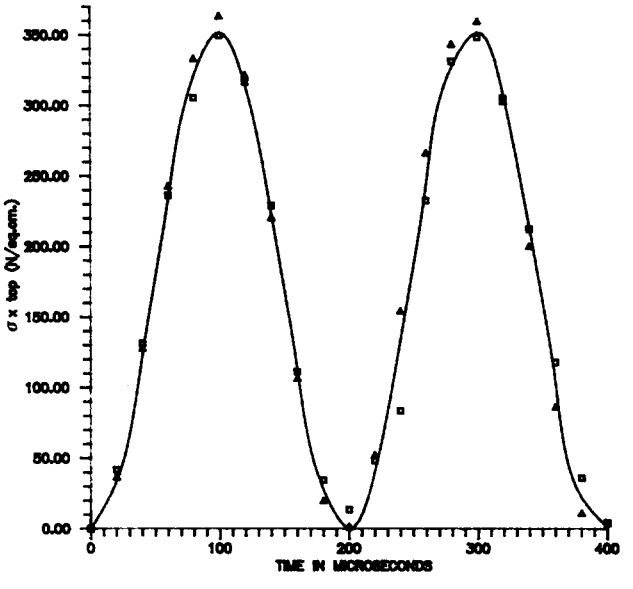

Fig. 6. Variation of normal bending stress σ_x (top) with time for a simply supported 0°/90° composite plate (Data 1) under suddenly applied spatially sinusoidal load. △, Mindlin;[17] □, host 11;[22] ——, present.

value is 10^8 N/m$^{1·5}$ for the present problem, r is the displacement of the projectile at any instant, w is the deflection of the point of impact at that instant and P is an exponential constant whose value is 1·5 in the present case.[28] The laminate consists of 0°/90°/0° stacking sequence and has clamped boundary conditions. The variation of the central deflection and forcing function with time and comparison with Ref. 28 are shown in Figs 7 and 8. The mesh pattern used is shown in Fig. 9.

Table 3. Comparison of peak of shear stresses τ_{xy} and τ_{xz} for a 0°/90° laminate (Example 3). ($\Delta t = 20$ μs.)

Time (μs)	τ_{xy} (N/cm^2)			τ_{xz} (N/cm^2)		
	Present	HOST [22]	CFS [17]	Present	HOST [22]	CFS [17]
20	2·7378	2·527	1·611	1·9003	3·451	2·252
40	10·200	10·41	8·506	6·8499	6·699	5·891
60	19·638	19·26	16·47	12·918	14·04	12·34
80	26·990	26·96	23·85	17·758	17·34	16·34
100	29·439	29·11	26·27	19·488	20·13	18·94
120	26·403	26·13	24·12	17·419	17·09	15·96
140	18·831	18·21	17·05	12·365	12·89	12·58
160	9·4164	9·079	8·848	6·3017	6·495	6·533
180	2·1796	2·016	2·029	1·5740	2·267	2·233
200	0·0063	0·159	0·248	0·0179	0·932	0·564

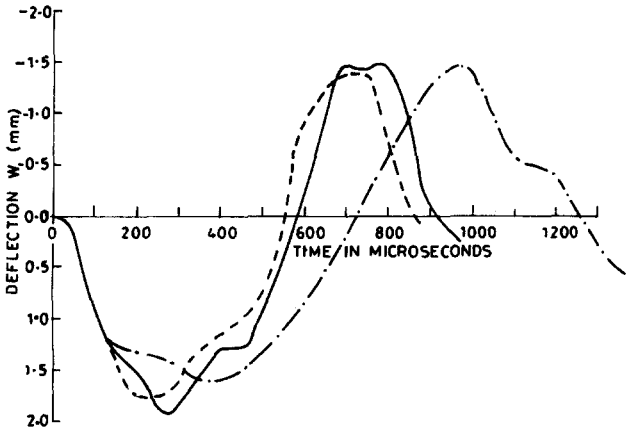

Fig. 7. Variation of central transverse deflection with time for a clamped 0°/90°/0° plate subjected to central impact loading of a blunt ended projectile (Data 3). (-·-) experimental;[28] (---) FOSD;[28] (——) present.

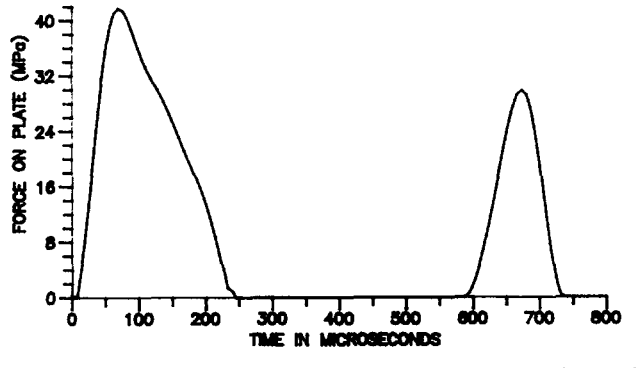

Fig. 8. Applied loading as a function of time for a clamped 0°/90°/0° plate subjected to central impact loading of a blunt ended projectile (Data 3).

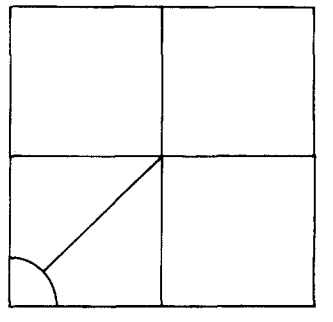

Fig. 9. Finite element mesh for projectile impact problem (Example 4).

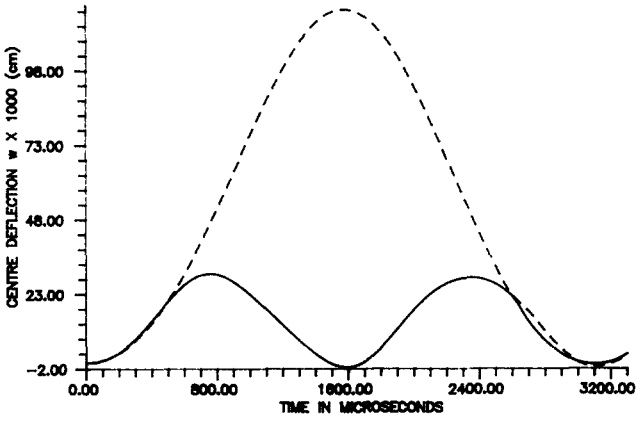

Fig. 10. Effect of shear rigidity of stiff layers on the central transverse deflection of 0°/45°/90°/CORE/90°/45°/30°/0° plate under suddenly applied pulse load. (——) with shear rigidity of face layers; (---) zero shear rigidity of face layers.

Example 5

A composite sandwich plate using DATA 2 is analysed here. The stacking sequence is 0°/45°/90°/CORE/90°/45°/30°/0°. Clamped boundary conditions have been taken and a uniformly distributed constant pulse load q_0 applied suddenly has been taken for computing the dynamic response using a 4×4 mesh discretization for full plate. The variation of central deflection and moment (M_x) are shown in Figs 10 and 11 respectively. The effect of reducing the shear rigidity terms (G_{13} and G_{23}) of the stiff layers to zero on the deflection and moment has also been studied and represented graphically in Figs 10 and 11. A considerable difference in deflection is observed in the absence of shear rigidity terms but there is

Table 4. Frequencies included in the analysis of 0°/45°/90°/core/90°/45°/30°/0° composite sandwich plate (Example 5) and their effect on the peak values of deflection and stress (σ_x) at the centre. ($\Delta t = 50$ μs.)

Nmode	Including shear rigidity of stiff layers (Reported values occurred at $t = 750$ μs)			Without considering shear rigidity of stiff layers (Reported values occurred at $t = 1600$ μs)		
	Frequency (rad/s)	$w \times 10^3$ (cm)	Moment (M_x) (N-cm/cm)	Frequency (rad/s)	$w \times 10^3$ (cm)	Moment (M_x) (N-cm/cm)
1	4017·060	30·2369	76·10813	2005·094	118·76643	77·79161
2	6207·508	30·2369	76·10813	2863·057	118·76643	77·79161
3	6246·972	30·2369	76·10813	3630·970	118·76643	77·79161
4	6551·602	30·2369	76·10813	3746·791	118·76643	77·79161
5	7292·884	30·2369	76·10813	3896·656	118·76076	77·78931
6	8771·887	30·2301	76·08175	4006·905	118·76076	77·78931
7	8858·167	30·2307	76·07724	4219·137	118·75700	77·78996
8	8996·416	30·2304	76·07641	4227·754	118·75700	77·78996
9	9450·460	29·9892	75·53368	4305·272	118·75701	77·78986

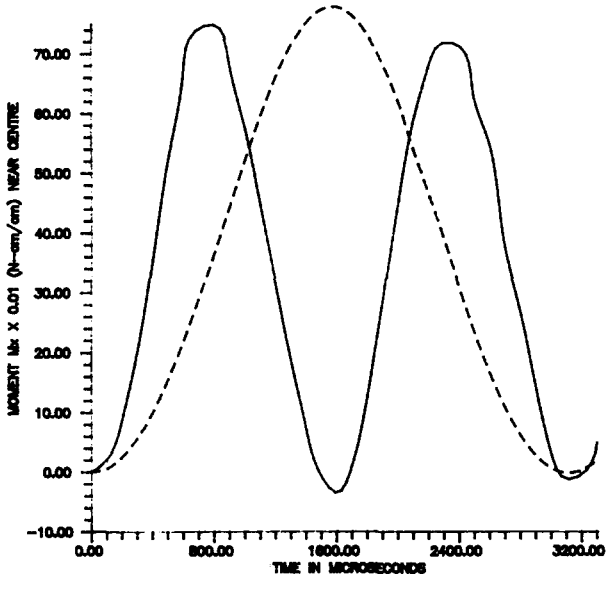

Fig. 11. Effect of shear rigidity of stiff layers on moment M_x for a 0°/45°/90°/CORE/90°/45°/30°/0° sandwich plate (Data 2) under a suddenly applied pulse load. (——) with shear rigidity of face layers; (– – –) without zero shear rigidity.

noticeable difference in the moment M_x as shown in these graphs. The frequencies that have been included in the dynamic analysis are given in Table 4 and the convergence of the peak values of the response when increasing the number of modes is also indicated.

6 CONCLUSIONS

Dynamic analysis of composite and sandwich plates is carried out using a higher order shear deformable theory. The method of mode superposition is used for computing the dynamic response. The present theory does not require the use of shear correction coefficient/s due to more realistic parabolic representation of cross-section deformation.

The method of mode superposition, being tried for the first time here in the field of transversely loaded composite laminates, has given very good results. At the same time, considerable saving in computation time is achieved in computer implementation for the same level of accuracy as compared to direct integration methods. The method is found to be very effective for the linear dynamic response of both symmetric and unsymmetric composite laminates.

REFERENCES

1. Reismann, H. & Lee, Y., Forced motion of rectangular plates. In *Developments in Theoretical and Applied Mechanics, 4*, ed. D. Frederick. Pergamon Press, New York, 1969, pp. 3–18.
2. Reismann, H., Forced motion of elastic plates. *ASME J. Appl. Mech.*, **35** (1968) 510–15.
3. Lee, Y. & Reismann, H., Dynamics of rectangular plates. *Int. J. Engng Sci.*, **7** (1969) 93–113.
4. Hinton, E., The dynamic transient analysis of axisymmetric circular plates by the finite element method. *J. Sound Vib.*, **4** (1976) 465–72.
5. Pica, A. & Hinton, E., Transient and pseudo-transient analysis of Mindlin plates. *Int. J. Numer. Meth. Engng*, **15** (1980) 189–208.
6. Pica, A. & Hinton, E., Further developments in transient and pseudo-transient analysis of Mindlin plates. *Int. J. Numer. Meth. Engng*, **17** (1981) 1749–61.
7. Yang, P. C., Norris, C. H. & Stavsky, Y., Elastic wave propagation in heterogeneous plates. *Int. J. Solids Struct.*, **2** (1966) 665–84.
8. Whitney, J. M. & Pagano, N. J., Shear deformations in heterogeneous anisotropic plates. *ASME J. Appl. Mech.*, **37** (1970) 1031–6.
9. Moon, F. C., One dimensional transient waves in anisotropic plates. *ASME J. Appl. Mech.*, **40** (1973) 485–90.
10. Wang, A. S. D., Chou, P. C. & Rose, J. L., Strongly coupled stress waves in heterogeneous plates. *AIAA J.*, **10** (1972) 1088–90.

11. Sun, C. T. & Whitney, J. M., Forced vibrations of laminated composite plates in cylindrical bending. *J. Acoust. Soc. Amer.*, **55** (5) (1974) 1003–8.
12. Sun, C. T. & Whitney, J. M., Dynamic response of laminated composite plates. *AIAA J.*, **13** (10) (1975) 1259–60.
13. Whitney, J. M. & Sun, C. T., Transient response of laminated composite plates subjected to transverse dynamic loading. *J. Acoust. Soc. Amer.*, **61** (1) (1977) 101–4.
14. Mindlin, R. D. & Goodman, L. F., Beam vibrations with time dependent boundary conditions. *ASME J. Appl. Mech.*, **17** (1950) 377–80.
15. Rock, T. & Hinton, E., Free vibration and transient response of thick and thin plates using the finite element method. *Int. J. Earthqu. Engng Struct. Dynam.*, **3** (1974) 51–63.
16. Akay, H. U., Dynamic large deflection analysis of plates using mixed finite elements. *Comput. Struct.*, **11** (1980) 1–11.
17. Reddy, J. N., On the solutions to forced response of rectangular composite plates. *ASME J. Appl. Mech.*, **49** (1982) 403–8.
18. Reddy, J. N., Dynamic (transient) analysis of layered anisotropic composite material plates. *Int. J. Numer. Meth. Engng*, **19** (1983) 237–55.
19. Pandya, B. N. & Kant, T., Finite element analysis of laminated composite plates using a higher order displacement model. *Compos. Sci. Technol.*, **32** (1988) 137–55.
20. Kant, T. & Mallikarjuna, Vibrations of unsymmetrically laminated plates using a higher order theory with C^0 finite element formulation. *J. Sound Vib.*, **134** (1) (1989) 1–16.
21. Kant, T., Ravichandran, R. V., Pandya, B. N. & Mallikarjuna, Finite element transient dynamic analysis of isotropic and fibre reinforced composite plates using a higher order theory. *Compos. Struct.*, **9** (4) (1988) 319–42.
22. Mallikarjuna & Kant, T., On transient response of laminated composite plates based on a higher order theory. *Proc. 3rd Int. Conf. on Recent Advances in Structural Dynamics*, 18–22 July, 1988, Southampton, UK, ed. M. Petyt, H. F. Wolfe & C. Mei. AFWAL-TR-88-3034/ ISBN 0-85432-2298, 1988, pp. 219–28.
23. Mallikarjuna & Kant, T., Dynamics of laminated-composite plates with a higher order theory and finite element discretization. *J. Sound Vib.*, **126** (3) (1988) 463–75.
24. Kant, T. & Mallikarjuna, Transient dynamic analysis of composite plates using 4-, 8- and 9-noded isoparametric quadrilateral elements. *Finite Elem. Anal. Design*, **6** (1989) 307–18.
25. Hinton, E., Rock, T. & Zienkiewicz, O. C., A note on mass lumping and related processes in the finite element method. *Int. J. Earthqu. Engng Struct. Dynam.*, **4** (1976) 245–9.
26. Jones, R. M., *Mechanics of Composite Materials*. McGraw-Hill, New York, 1975.
27. Khatua, T. P. & Cheung, Y. K., Bending and vibration of multilayer sandwich beams and plates. *Int. J. Numer. Meth. Engng*, **6** (1973) 11–24.
28. Aggour, H. & Sun, C. T., Finite element analysis of a laminated composite plate subjected to a circularly distributed central impact loading. *Comput. Struct.*, **28** (1988) 729–36.